International Conference on Computer, Communication, Chemical, Materials and Electronic Engineering (IC4ME2), 11-12 July, 2019

CPW-fed Ultra-wideband Flexible Disc Monopole Antenna Design for Early Detection of Brain Stroke

Md. Ashikur Rahman
Dept. of Electronics & Communication Engineering (ECE)
Khulna University of Engineering & Technology (KUET)
Khulna-9203, Bangladesh
ashikur.rahman0809@gmail.com

Md. Foisal Hossain
Dept. of Electronics & Communication Engineering (ECE)
Khulna University of Engineering & Technology (KUET)
Khulna-9203, Bangladesh
foisalkuet@yahoo.com

***Abstract*—The desire for wearable ultra-wideband antennas has grown up rapidly in recent years. This paper presents a wearable ultra-wideband (UWB) antenna fed by a coplanar waveguide (CPW) on paper substrate and analysis of its performance for early detection of brain stroke. A very thin sheet of paper is considered as substrate in order to make the antenna flexible, wearable, low-cost and environment friendly. The antenna shows reflection co-efficient of –10 dB or less at frequencies between 1.91 GHz to 34.45 GHz. It covers the 2.36–2.4 GHz MBAN (Medical Body Area Network) band, 2.4–2.5 GHz ISM (Industrial, Scientific and Medical) band, 3.1–10.6 GHz UWB and internet of things (IoT) frequency bands and 5G communication bands. Specific Absorption Rate (SAR) is calculated placing the antenna to a 7-layer human head model only 5 mm apart in order to check the compatibility of the antenna for wearable applications. Improvement in SAR is also shown comparing with other antennas. Improvement of SAR and other simulation results of the proposed antenna make it suitable for wearable applications.**

Keywords—low-cost, inkjet printing, ultra-wideband (UWB), specific absorption rate (SAR), brain stroke detection

I. INTRODUCTION

Predilection for ultra-wideband wearable technologies has increased now-a-days. Also, the importance of low-cost, flexible and environment friendly antennas has risen up. In that case, using paper as substrate can be low-cost, flexible and easily disposable. In the process of fabricating antennas, to avoid lengthy process and cost, inkjet printing technology is one of the very useful technologies as it is a one-step process. Applications in the human body proximity require flexible antennas for comfortable movements of the human body.

Many research papers on ultra-wideband flexible and low-cost antenna have been published in recent years. A circular disc monopole antenna is studied in [1], but no specific application of the antenna is mentioned. An elliptical disc monopole antenna on Kapton polyimide substrate is designed in [2] with half circular modified ground on other side of the elliptical disc. The cost of the ink must be reduced in order to design a cheaper antenna. Silver nanoparticles ink is used in [3–6, 8–10] which is costlier compared to copper nanoparticles ink. In free space and with a human model a paper substrate based monopole antenna is tested in [6], but no geometry of the human phantom model with the antenna is shown. A star shaped patch antenna on a paper substrate is presented in [7]. It is not ink-jet printed; rather, a copper tape is used as radiating element. A wide-band monopole antenna is presented in [10] without mentioning any specific application of the antenna.

A miniature size ultra-wideband antenna is presented in [11] for portable stroke detection but, SAR calculation is not considered. A compact 3-D unidirectional UWB antenna is presented in [19] without considering SAR. A flexible monopole antenna with directional radiation is presented in [17] for stroke detection along with the SAR calculation at different power levels. But, the SAR for this antenna can be reduced.

In this paper, the presented antenna has a very large bandwidth comparable to other UWB antennas which covers the ISM band, UWB band and beyond. Copper nanoparticles ink is considered for the inkjet printer which reduces the cost of silver nanoparticles ink. An elaborate discussion and analysis of human head model which many research papers only have mentioned but have not elaborated. SAR values are calculated for different frequencies and power levels which are comparatively lower than that of other research papers. Finally, the operating bandwidth comparison is given in a tabulated form.

In section II, geometry of the designed antenna and 7-layer human head model are presented. Simulation results of the antenna are presented in section III. In section IV, the calculation of SAR values are shown for different power levels and analyzed for different frequencies. Finally, it is concluded in section V.

II. ANTENNA DESIGN AND HUMAN HEAD MODEL

In this section, the geometry of the antenna is discussed. Also, model of various human head layers are designed and discussed.

A. Antenna Design

In this section, a CPW-fed circular disc monopole ultra-wideband (UWB) antenna is designed. A thin sheet of paper is used as substrate with relative permittivity (ε_r) of 2.85 and loss tangent (tan δ) of 0.05. The length (L) and width (W) of the antenna is 67 mm and 47 mm respectively. Table I shows the values of the antenna parameters. The structure of the proposed 50Ω CPW-feed patch antenna with ground on the same side is shown in Fig. 1. To feed the antenna, SMA (SubMiniature version A) connector is used. It is very important to match the impedance of SMA connector and CPW-feed line as the better the antenna is matched with feeding line the better the radiation characteristics. The two slots between the two ground plates and the feeding line are denoted by 'g' which is responsible for the radiation performance. The circular patch is optimized to radius (R) of 13.35 mm. The paper sheet has a thickness (h) of 0.254 mm.

978-1-7281-3060-6/19/$31.00 ©2019 IEEE

TABLE I. DIMENSIONS OF THE PROPOSED ANTENNA

Antenna Dimensions	Value (mm)	Antenna Dimensions	Value (mm)
W	47	R	13.35
L	67	g	0.2
W_f	2.32	h	0.254
W_g	22.14	t	0.035

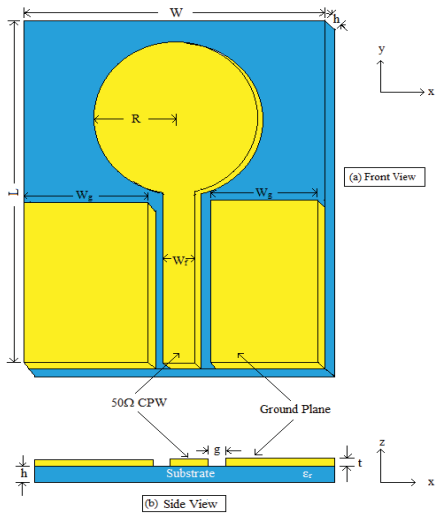

Fig. 1. Antenna structure. (a) Front view; (b) Side view.

B. Modelling of Human Head

A 7-layered human head model is designed in this section including layers of skin (dry), fat, muscle, skull, dura, cerebro spinal fluid and brain. For computational simplicity and accuracy, the 7-layered model is chosen. Wearable antenna design needs a complete understanding of the interaction between antenna and head model and the electrical properties of body tissues. The proposed antenna placed to the 7-layered model with thickness of 2, 2, 4, 10, 1, 2 and 10 mm for skin (dry), fat, muscle, skull, dura, cerebro spinal fluid and brain respectively. The electrical properties such as, permittivity (ε_r) and conductivity (σ) of different layers for a homogeneous cylindrical head model of 100 mm radius is collected [13, 14]. Fig. 2 shows the antenna placed close to the 7-layer human head model of the SAM (Specific Anthropomorphic Mannequin) phantom for calculation of SAR.

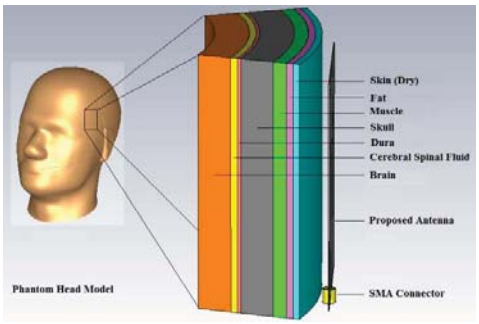

Fig. 2. 7-layered human head model with proposed antenna.

III. ANTENNA SIMULATION RESULTS

Antenna simulation results are discussed in this section.

A. Return Loss

In this section, a return loss graph of the antenna without and with human head is shown. In Fig. 3 (b), it is seen that return loss curve shifted in the left side as the antenna is placed close to the head model. The first resonant frequency is shifted towards 2.1 GHz from 3.2 GHz. From Fig. 3 (a), it is seen that the antenna can operate in the range of 1.91 GHz to 34.45 GHz with more than –10 dB return loss. For the ease of analysis, 1 GHz to 11 GHz range of frequency is considered during simulation.

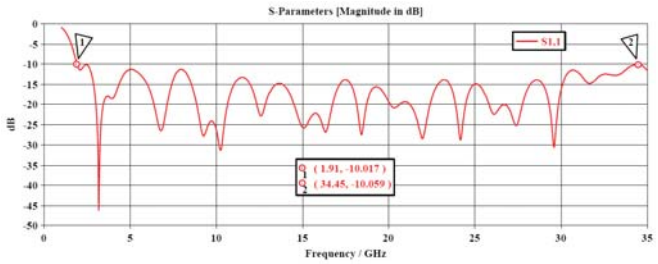

(a)

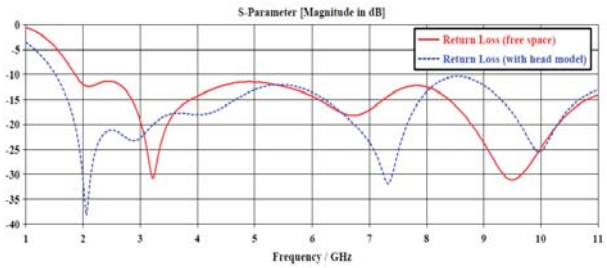

(b)

Fig. 3. Return loss graph (a) in free space; (b) ccomparison between free space and with head model.

B. Antenna Gain

In this section, graph of realized gain over frequency of the antenna without and with head model is shown in Fig. 4. It can be realized that in lower frequencies, the antenna gain is higher in free space than that of the antenna placed near head model. On the other hand, the antenna gain is higher without head model than that of the antenna placed near head model. However, the antenna can be in operation with nearly a stable gain both with and without human head model.

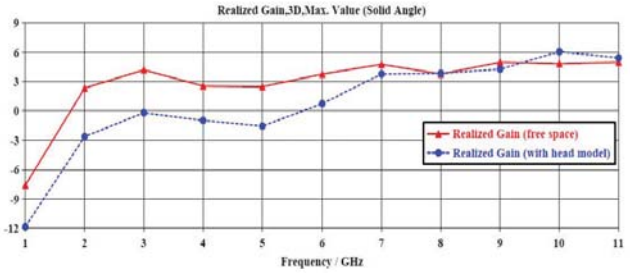

Fig. 4. Realized Gain over frequency of the antenna with and without head model.

C. Radiation Efficiency

In this section, radiation efficiency graph and total antenna efficiency with and without head model is shown in Fig. 5. The antenna has an efficiency of more than 90% without head model. On the other hand, the antenna efficiency reduces as the antenna is close to the head model.

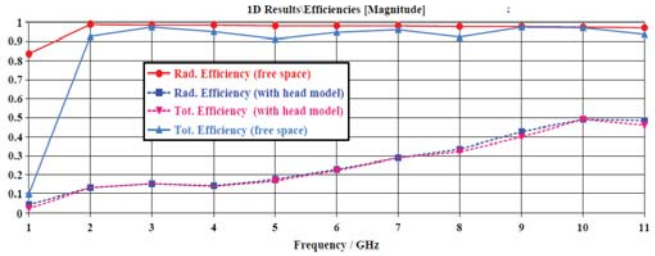

Fig. 5. Radiation efficiency and total efficiency in free space and with head model.

D. Radiation Pattern

This section shows the antenna radiation patterns at 2 GHz, 3 GHz and 4 GHz frequency for both without and with head model. Fig. 6 shows that the antenna has an omni-directional radiation pattern without head model. On the other hand, with the head model, the main lobe of the antenna radiation is directed towards the perpendicular direction of the head model as a major part of the radiation is reflected by the head. The solid red lines in the radiation pattern graph indicate the radiation patterns in free space and dotted blue lines indicate the radiation patterns with head model. In Fig. 7, 3D radiation pattern at 2 GHz, 3 GHz and 4 GHz is shown for both in free space and with head model. It is clear that when the antenna is stimulated near head model a major part of radiation reflects in the negative z-axis. Also, it can be seen that the antenna realized gain has reduced.

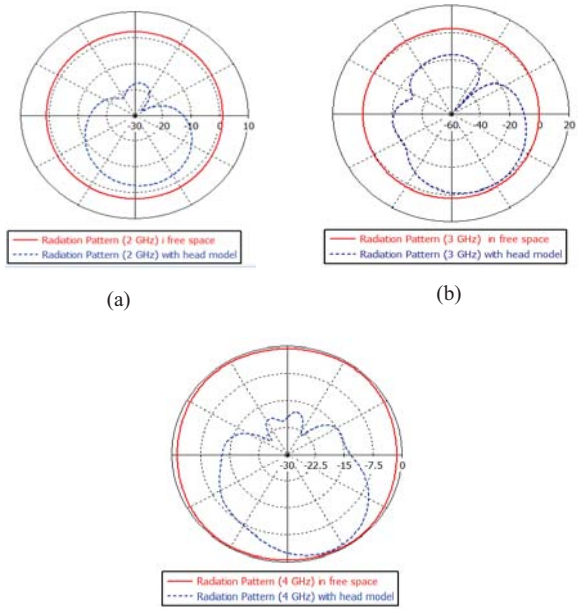

Fig. 6. Radiation patterns without and with human head at (a) 2 GHz; (b) 3 GHz; (c) 4 GHz

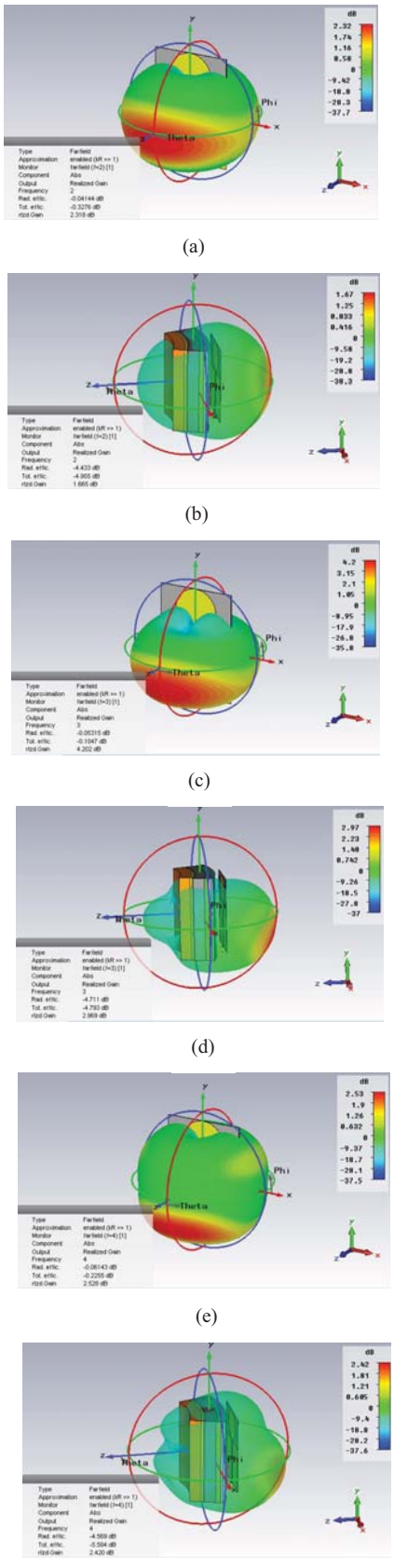

Fig. 7. 3D Radiation Pattern at (a) 2 GHz without head; (b) 2 GHz with head; (c) 3 GHz without head; (d) 3 GHz with head; (e) 4 GHz without head; (f) 4 GHz with head model.

IV. SAR Calculation and Analysis

In this section, SAR values are calculated and analyzed. As the proposed wearable antenna is placed near human head (5 mm distance) SAR values must be considered for testing exposure limit of the human body. SAR values are calculated for 10g and 1g of tissues. The exposure limit is 2.0 W/kg for 10g of tissues defined by the International Commission on Non-Ionizing Radiation Protection (ICNIRP). Also, the FCC defined limit is 1.6 W/kg averaged over 1g of tissue [15]. At different frequencies, maximum SAR for 10mW power is shown in Table II. Maximum stimulated power considered is 10mW. –41.3 dBm/MHz (75nW/MHz) is the maximum allowable Power Spectral Density (PSD) in UWB range [12]. For 2.5 GHz frequency, stimulated power is 10mW and accepted power is 6.4mW. SAR value is 0.079 W/kg for 10g of tissues and 0.163 W/kg for 1g of tissues. For all other frequencies, the maximum SAR values are within the regulated level. The antenna is set at only 5 mm distance from the head so that the radiation signal can penetrate deep into the head for better performance. Fig. 8 shows the SAR values at 2.5 GHz for 1mW, 10mW and 100mW respectively. Comparison of SAR values at 0 dB, 10 dB and 20 dB power levels for 1.5 GHz to 4 GHz frequencies between proposed antenna and the antenna designed in [17] is shown in Fig. 9. The proposed antenna shows comparatively low SAR calculated than the reference antenna for same distance between antenna and head model. Table IV shows the comparison among various UWB antennas. The proposed antenna can operate in the range of 1.91–34.45 GHz, which is comparable to the enlisted antennas. Size of the proposed antenna is also comparable. In addition, this antenna has a stable gain of 3–6 dB over the whole frequency range. Moreover, it has an efficiency of 90%–95% over the range of frequencies.

TABLE II. MAX. SAR AT DIFFERENT FREQUENCIES AT 5MM DISTANCE FROM HEAD MODEL

Frequency (GHz)	Stimulated Power (mW)	Accepted Power (mW)	Absorbed Power (mW)	IEEE/IEC 62704-1	
				Max. SAR (10g) in W/kg	Max. SAR (1g) in W/kg
1.5	10	6.4	5.3	0.085	0.197
2.0	10	8.9	5.6	0.090	0.195
2.5	10	9.1	5.0	0.079	0.163
3.0	10	9.8	6.4	0.084	0.195
3.5	10	9.6	6.4	0.124	0.312
4.0	10	7.9	5.0	0.153	0.385

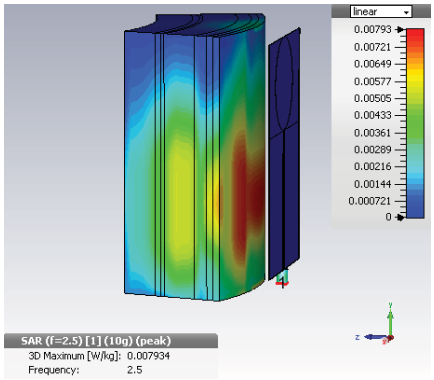

(a)

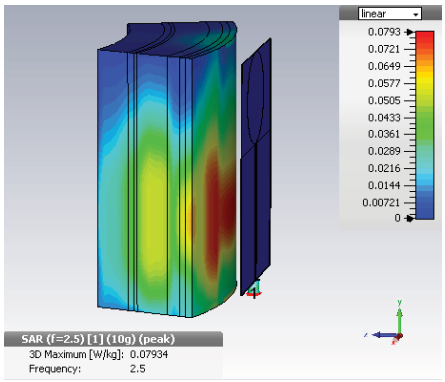

(b)

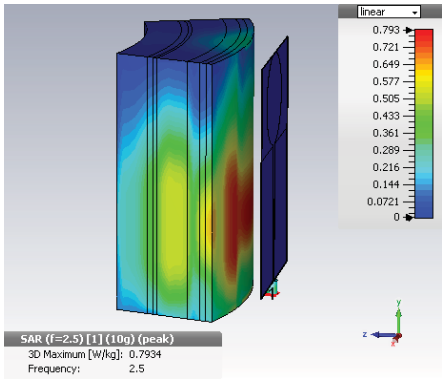

(c)

Fig. 8. SAR values at 2.5 GHz for power of (a) 1mW; (b) 10mW; (c) 100mW;

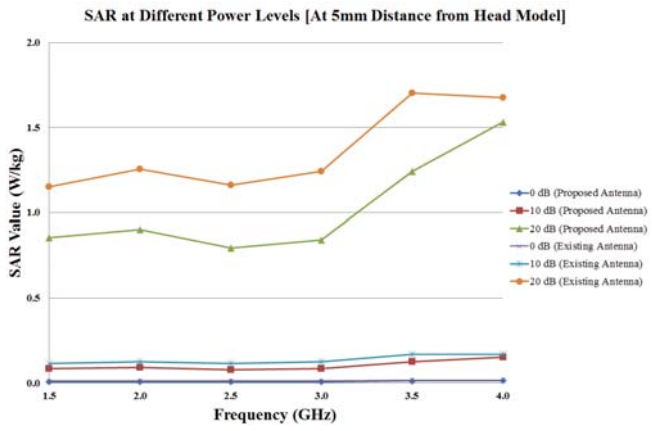

Fig. 9. Comparison of SAR values between proposed antenna and the antenna presented in [17].

TABLE III. COMPARISON AMONG UWB ANTENNAS

References	Antenna Size (mm^2)	Bandwidth (GHz)
[1]	67×47	2.64–20
[2]	30×35	3.1–12
[3]	60×45	1.5–2.7, 5.1–11
[4]	51×31	3.2–10.3
[5]	58×58	1.5–16
[6]	127×87	2.4–2.5
[7]	40×23	2.45–6
[8]	30×33	2.3–15.2
[9]	79.8×94.6	2.3–12
[10]	49×28	2–10
[11]	40×40	1–4
[17]	70×30	1.3–3.5
[18]	74×42	5–10
[19]	80×15	1–2.3
[20]	33.1×32.7	3.2–30
Proposed Antenna	**67×47**	**1.91–34.45**

V. BENDING TEST

The designed antenna is bent along its width at 25 mm and 50 mm cylindrical radius. Fig. 10 (a) and 10 (b) shows the bending structure of the antenna and variation in reflection parameters. It can be understood that there is slight variation in reflection coefficient due to bending.

(a)

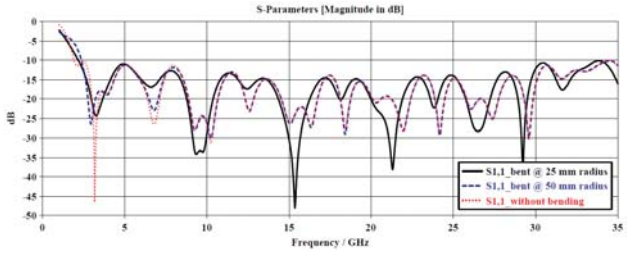

(b)

Fig. 10. (a) Bent structure; (b) variation in reflection coefficient.

VI. EARLY STROKE DETECTION

The proposed antenna is placed near a cylindrical head phantom at only 5 mm distance to set two different arrangements. In the first setup, there is no stroke model in the arrangement while in the second setup a stroke model is added for the analysis. This arrangement acts as a technique of mono-static radar. When there is no stroke, the incident signal, *i1* is reflected and reflected signal, *o1.1* is obtained. Similarly, when there is a stroke, the incident signal, *i2* is reflected and reflected signal, *o2.2* is obtained. After observing these two signals, it can be determined that the reflected signal level of the 2nd setup with stroke is higher than the reflected signal level of the 1st without stroke. Observing the reflected signal level, primarily it can be predicted and detected whether there is any stroke or not. Fig. 11 (a) shows the antenna arrangement with the head model. Fig. 11 (b) shows the reflected signal levels with and without stroke models.

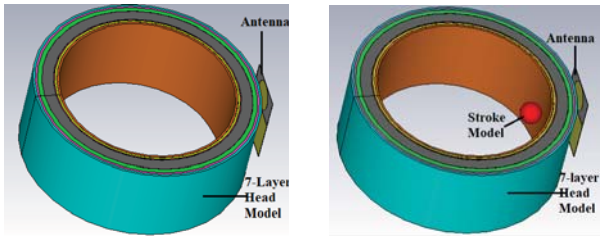

(a)

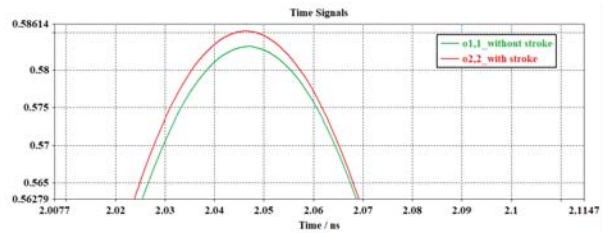

(b)

Fig. 11. (a) Antenna arrangement with head model; (b) reflected signal levels.

VII. CONCLUSION

The design of a flexible, low-cost, wearable inkjet printable UWB monopole disc antenna is discussed in detail in this paper. Dimensions of the antenna and its geometry are discussed along with seven layers of the head model. Copper nanoparticles are considered as the radiating elements instead of silver nanoparticles in order to reduce the cost. The return loss curve is shown in a figure. In another figure, the return loss comparison curve between free space and with human head model is depicted. Also, realized gain, antenna efficiency and radiation patterns are discussed with respective figures. The calculation of SAR values are shown for different power levels and analyzed for different frequencies. All the values are listed in a table. The calculated values of SAR at 2.5 GHz for 1mW, 10mW and 100mW power are shown in a figure. It is also shown that calculated SAR values are comparable to existing antenna presented in [17] for the same distance between the head model and the antenna at 0dB, 10dB and 20dB power levels. The antenna has 3–6 dB gain and an operating frequency of 1.91–34.45 GHz. A comparison of operating frequencies among different UWB antennas is listed in a table. This antenna can operate over a very large bandwidth comparable to other UWB antennas along with a stable gain and SAR values at different frequencies within the acceptable limit set by FCC and ICNIRP. The evidence above shows that the proposed CPW-fed UWB low-cost, flexible circular disc monopole antenna on paper substrate is compatible for early brain stroke detection.

REFERENCES

[1] J. Liang, L. Guo, C.C. Chiau, X. Chen and C.G. Parini, "Study of CPW-fed circular discmonopole antenna for ultra wideband applications," IEE Proceedings of Microwave Antennas Propaation., vol. 152, no. 6, December 2005

[2] A. A. Adam, S. K. A. Rahim, K. G. Tan, and A. W. Reza, "Design of 3.1–12 GHz printed elliptical disc monopole antenna with half

circular modified ground plane for UWB application," Wireless Personal Commununications, vol. 69, pp. 535–549, 2013

[3] H. A. Elmobarak, S. K. A. Rahim, M. Himdi, X. Castel, and T. A. Rahman, "Low cost instantly printed silver nano ink flexible dual-band antenna onto paper substrate," 11th European Conference on Antennas and Propagation (EUCAP), 2017

[4] A. R. Maza, B. Cook, G. Jabbour, and A. Shamim, "Paper-based inkjet-printed ultra-wideband fractal antennas," IET Microwaves, Antennas & Propagation, April 2012

[5] G. Shaker, S. Safavi-Naeini, N. Sangary, and M. M. Tentzeris, "Inkjet printing of ultrawideband (UWB) antennas on paper-based substrates," IEEE Antennas and Wireless Propagation Letters, vol. 10, 2011

[6] S. Kim, Y. Ren, H. Lee, A. Rida, S. Nikolaou, and M. M. Tentzeris, "Monopole antenna with inkjet-printed EBG array on paper substrate for wearable applications," IEEE Antennas and Wireless Propagation Letters, vol. 11, 2012

[7] W. N. N. W. Marzudi, Z. Z. Abidin, S. H. Dahlan, K. N. Ramli, and M. R. Kamarudin, "Performance of star patch antenna on a paper substrate material," ARPN Journal of Engineering and Applied Sciences, vol. 10, no. 19, October, 2015

[8] H. R. Khaleel "Design and fabrication of compact inkjet printed antennas for integration within flexible and wearable electronics," IEEE Transactions on Components, Packaging and Manufacturing Technology, vol. 4, no. 10, October 2014

[9] B. S. Cook, and A. Shamim, "Inkjet printing of novel wideband and high gain antennas on low-cost paper substrate," IEEE Transactions on Antennas and Propagation, vol. 60, no. 9, September 2012

[10] H. P. Phan, T. P. Vuong, P. Benech, P. Xavier, P. Borel, and A. Delattre, "Novel ultra-wideband "Robe" antenna on high-loss paper substrate," IEEE International Symposium on Antennas and Propagation & USNC/URSI National Radio Science Meeting, 2017, San Diego, CA, USA

[11] Yizhi Wu, Mingsai Wang, and Sheng Ye, "A campact ultra-wideband antenna for stroke detection," IEEE International Conference on Microwave and Millimeter Wave Technology (ICMMT), vol. 2, pages: 546–548, 2016

[12] "First Carry forward and Order: Revision of part 15 of the commission's rules regarding UWB transmission systems," FCC 02-48A1, Federal Communications Commission, February 2002

[13] (2016) The FCC website. [Online]. Available: https://www.fcc.gov/general/body-tissue-dielectric-parameters

[14] C. Gabriel, S. Gabriely, and E. Corthout, "The dielectric properties of biological tissues: I. Literature survey," Physics in Medicine and Biology, 41, pp. 2231–2249, 2016

[15] IEEE standard for safety levels with respect to human exposure to the radio frequency electromagnetic fields 3 kHz to 300 GHz, IEEE Std. C95.1., 2005

[16] "Guidelines on limits on exposure to radio frequency electromagnetic fields in the frequency range from 100 kHz to 300 GHz", ICNIRP Std. 1998, Health Physics, Vol. 54, No. 1, pp. 115–123

[17] M. S. R. Bashri, T. Arslan1, and W. Zhou, "Flexible antenna array for wearable head imaging system," 11th European Conference on Antennas and Propagation (EUCAP), 2017

[18] H. Zhang, B. Flynn, A. T. Erdogan, and T. Arslan, "Microwave imaging for brain tumour detection using an UWB Vivaldi Antenna Array," Loughborough Antennas & Propagation Conference, 2012

[19] A. T. Mobashsher, and A. M. Abbosh, "Development of compact three-dimensional unidirectional ultra-wideband antennas for portable microwave head imaging systems," IEEE International Symposium on Antennas and Propagation & USNC/URSI National Radio Science Meeting, 2015

[20] Saha, T. K., Knaus, T. N., Khosla, A., and Sekhar, P. K., "A CPW-fed flexible UWB antenna for IoT applications," Microsystem Technologies, 2018

978-1-7281-3060-6/19/$31.00 ©2019 IEEE